AGU PUBLICATIONS

JGR

Journal of Geophysical Research: Atmospheres

RESEARCH ARTICLE
10.1002/2017JD027398

Key Points:
- UTLS ozone accounts for important differences in the CMIP5 GCM simulations
- GCM experiment verifies its strong influences on high cloud and stratospheric temperature and water vapor
- These rapid adjustments in response to ozone strongly modify its global radiative forcing

Supporting Information:
- Supporting Information S1

Correspondence to:
Y. Xia,
yan.xia3@mail.mcgill.ca

Citation:
Xia, Y., Huang, Y., & Hu, Y. (2018). On the climate impacts of upper tropospheric and lower stratospheric ozone. *Journal of Geophysical Research: Atmospheres*, *123*, 730–739. https://doi.org/10.1002/2017JD027398

Received 6 JUL 2017
Accepted 21 DEC 2017
Accepted article online 28 DEC 2017
Published online 17 JAN 2018

On the Climate Impacts of Upper Tropospheric and Lower Stratospheric Ozone

Yan Xia[1,2], Yi Huang[2], and Yongyun Hu[1]

[1]Department of Atmospheric and Oceanic Sciences, Peking University, Beijing, China, [2]Department of Atmospheric and Oceanic Sciences, McGill University, Montreal, Quebec, Canada

Abstract The global warming simulations of the general circulation models (GCMs) are generally performed with different ozone prescriptions. We find that the differences in ozone distribution, especially in the upper tropospheric and lower stratospheric (UTLS) region, account for important model discrepancies shown in the ozone-only historical experiment of the Coupled Model Intercomparison Project Phase 5 (CMIP5). These discrepancies include global high cloud fraction, stratospheric temperature, and stratospheric water vapor. Through a set of experiments conducted by an atmospheric GCM with contrasting UTLS ozone prescriptions, we verify that UTLS ozone not only directly radiatively heats the UTLS region and cools the upper parts of the stratosphere but also strongly influences the high clouds due to its impact on relative humidity and static stability in the UTLS region and the stratospheric water vapor due to its impact on the tropical tropopause temperature. These consequences strongly affect the global mean effective radiative forcing of ozone, as noted in previous studies. Our findings suggest that special attention should be paid to the UTLS ozone when evaluating the climate effects of ozone depletion in the 20th century and recovery in the 21st century. UTLS ozone difference may also be important for understanding the intermodel discrepancy in the climate projections of the CMIP6 GCMs in which either prescribed or interactive ozone is used.

1. Introduction

Stratospheric ozone has undergone considerable variations over the past decades (Roth et al., 2014; Solomon, 1999). Particularly, a severe depletion is observed in the Antarctic lower stratosphere where chlorofluorocarbons (CFCs) catalytically destroy ozone in the last several decades in the twentieth century (Solomon, 1999). The Antarctic ozone depletion has significant impacts on the Southern Hemispheric (SH) tropospheric and surface climate, such as the position of westerly jet and storm tracks, clouds, precipitation, and surface temperature (Bitz & Polvani, 2012; Kang et al., 2011; Son et al., 2009; Thompson et al., 2011; Turner et al., 2009). The recovery of ozone in the 21st century is expected to have opposite effects on climate (Arblaster et al., 2011; Perlwitz et al., 2008; Son et al., 2008). Ozone depletion in the Arctic lower stratosphere is weaker except for some extreme ozone loss years (Hu & Xia, 2013; Manney et al., 2011). And it may also have important impacts on tropospheric climate (Cheung et al., 2014; Karpechko et al., 2014; Xie et al., 2016) and Arctic polar vortex position (Zhang et al., 2016).

Besides chemistry, stratospheric ozone is also influenced by dynamics. General circulation model (GCM) simulations project a robust strengthening of the Brewer-Dobson circulation (BDC) in response to the increase of greenhouse gases (Butchart et al., 2006; Lin & Fu, 2013; Shepherd & McLandress, 2011; Xie et al., 2008). There is also evidence of strengthening of the BDC since 1980 in the observation (Fu et al., 2015; Hu & Fu, 2009). The strengthening of the BDC would decrease the abundance of tropical lower stratospheric ozone through transporting more air mass of less ozone from the tropical troposphere into the stratosphere, and an increase of ozone in the extratropics by the increase of poleward transport (Bekki et al., 2011). It is found that this process, acting as stratospheric ozone feedback, tends to reduce SH tropospheric circulation response (such as the shift of midlatitude jet) to increased CO_2 (Chiodo & Polvani, 2017).

Interestingly, in a set of experiments based on the Community Atmosphere Model, CAM3 (Collins et al., 2006), of the National Center of Atmospheric Research (NCAR), Xia et al. (2016) find that a stratospheric ozone perturbation may significantly change global high cloud fraction, which in turn strongly affects the radiative forcing of the ozone perturbation. The high cloud change mainly results from the changes in relative humidity and static stability in the upper troposphere and lower stratosphere (UTLS) (Hansen et al., 1997;

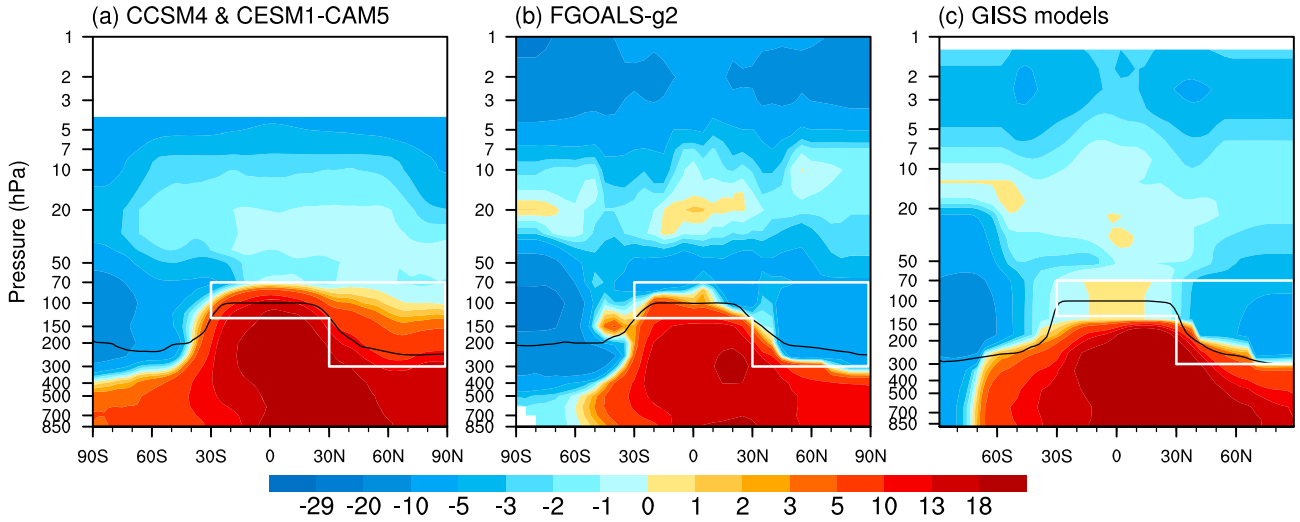

Figure 1. Annual and zonal mean fractional change of ozone from 1955 to 2000 ($[O_3(2000) - O_3(1955)]/O_3(2000) \times (100/1.8)$) prescribed in (a) NCAR CCSM4 and CESM1-CAM5, (b) FGOALS-g2, and (c) GISS-E2-R and GISS-E2-H. Units: percent. The black lines indicate the corresponding tropopause for each model. The UTLS regions subject to important ozone difference concerned here are marked by white polygons.

Hodnebrog et al., 2014; Xia et al., 2016). The severity of the forcing adjustment by high cloud simulated by CAM3 motivates us to further verify the robustness and impacts of the high cloud repsonse to ozone change, especially in the UTLS region.

Because of the large ozone variability in the UTLS region, there are significant uncertainties in both the observed and simulated UTLS ozone trends (Harris et al., 2015; Steinbrecht et al., 2017). Intermodel comparisons show large differences in UTLS ozone, which mainly depend on the details of the presentation of underlying processes (Gettelman et al., 2010; Hegglin et al., 2010; Ploeger et al., 2010; Riese et al., 2012). The historical experiments of Coupled Model Intercomparison Project Phase 5 (CMIP5) (Taylor et al., 2012) were performed with differently prescribed UTLS ozone changes (see discussions in the following section). This provides an opportunity to delineate the climate adjustments in response to the UTLS ozone. To verify our findings from the Coupled Model Intercomparison Project Phase 5 (CMIP5) analysis, we conduct additional sensitivity experiments with a newer version of the NCAR GCM, CAM5 (Neale et al., 2010) using contrasting ozone perturbations similar to those in the CMIP5 models. In this study, we will use the archived simulations of a few GCMs of the CMIP5, as well as CAM5, to investigate the atmospheric adjustments in response to the stratospheric ozone perturbation. In the following sections, we will describe the CMIP5 analysis, the CAM5 experiments, and the results in order.

2. Models and Data

2.1. CMIP5 Experiments

To isolate the ozone impact, ozone-only forcing runs are required. The natural and anthropogenic forcings, including solar, volcanic, greenhouse gases, aerosols, and land use, except for stratospheric and tropospheric ozone are fixed at preindustrial condition (year 1850) in the simulations (referring to the website: http://www.cesm.ucar.edu/CMIP5/forcing_information/). These runs are available from five CMIP5 models: NCAR CCSM4 and CESM1-CAM5, FGOALS-g2, and GISS E2-R, and E2-H. The simulations of these models are performed with three different historical ozone data sets (see detailed descriptions in Table 1 in Eyring et al., 2013). As shown in Figure 1, all these models show long-term ozone reduction in the upper stratosphere and depletion in the Antarctic lower stratosphere. The spatial correlation between the NCAR models and FGOALS-g2 is 0.92. And it is about 0.86 between the NCAR and Goddard Institute for Space Studies (GISS) models. However, different from the FGOALS-g2 and GISS models, the NCAR models show noticeable increases of ozone in the tropical tropopause region and the extratropical lower stratosphere in the Northern Hemisphere (NH). Hence, we can infer the effects of UTLS ozone by comparing the NCAR models with the others.

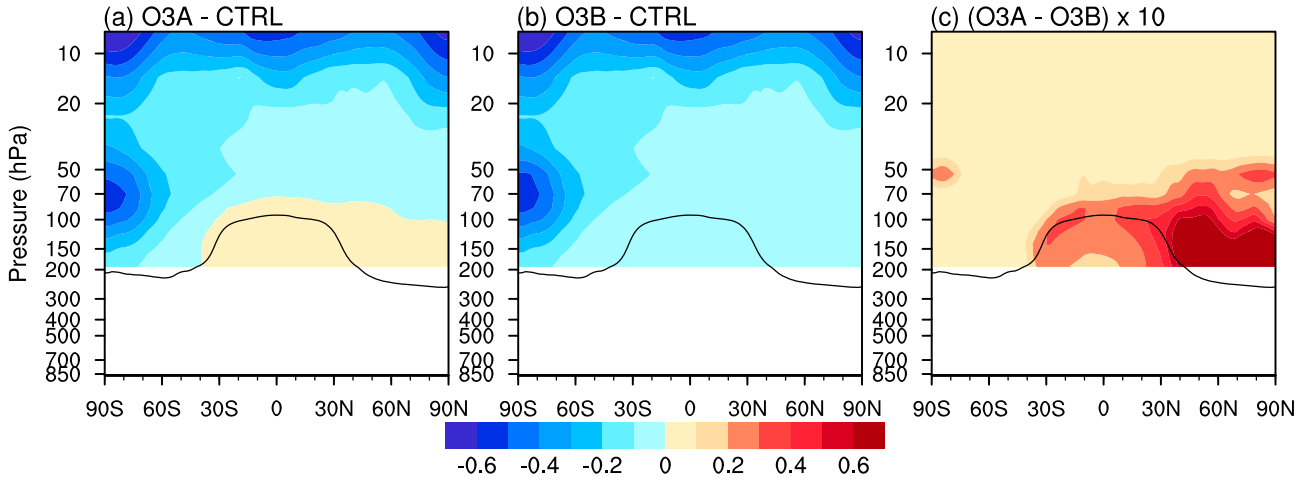

Figure 2. Annual and zonal mean differences of the volume mixing ratio of ozone between the (a) O3A and control experiments, (b) O3B and control experiments, and (c) (difference between the O3A and O3B experiments) × 10. Units: ppmv.

2.2. GCM Experiments

To verify the effects of the UTLS ozone, we also perform sensitivity experiments with different ozone prescriptions using an atmospheric GCM. The model used here is the NCAR CAM5. The CAM5 is configured at 1.9° × 2.5° horizontal resolution with 30 vertical levels. The prescribed ozone here is from the data set described by Lamarque et al. (2010, 2011) and is the same as used by the NCAR models in CMIP5 historical experiments.

A set of experiments are performed using CAM5, with greenhouse gases, aerosols, solar constant, sea ice, and sea surface temperature (SST), except for stratospheric ozone, fixed at year-2000 values. A control experiment is performed with ozone prescribed to year-1955 values. A forcing experiment, O3A, has settings similar to the control experiment, except that the ozone concentration above 200 hPa is prescribed with year-2000 values; ozone below 200 hPa is maintained at year-1955 level to eliminate the impacts of tropospheric ozone change. The ozone difference between the O3A and control experiments is shown in Figure 2a. Comparing O3A to control, we can infer the effects of ozone change above 200 hPa as prescribed in the NCAR GCMs in CMIP5 experiments. The ozone depletion used in another experiment, O3B, is obtained by taking the absolute value of the difference between 1955 and 2000 (Figure 2b). The difference between the O3B and control experiments mimics the simulations of the FGOALS-g2 and GISS models in CMIP5 experiments. We can then isolate the effect of the UTLS ozone by comparing the O3A and O3B experiments. The global mean value of the column ozone in the control experiment is about 399.5 Dobson units (DU). The global mean ozone perturbations in the O3A and O3B experiments are −11.7 and −15.3 DU, respectively, which are similar to those in the CMIP models (Eyring et al., 2013).

3. Results

3.1. CMIP5

Figure 3 shows the temperature, cloud, and water vapor changes from 1950–1959 to 1995–2004 in CCSM4, CESM1-CAM5, FGOALS-g2, GISS-E2-H, and GISS-E2-R in the CMIP5 ozone-only historical experiments. All these models show weak tropospheric warming and strong cooling in large parts of stratosphere in response to the ozone changes as shown in Figure 1.

The stratospheric temperature changes simulated by these GCMs can be well explained by the radiative heating/cooling of ozone. Stratospheric cooling occurs in the tropical and SH lower stratosphere, which is consistent with the stratospheric ozone reduction and associated reduction in shortwave (SW) heating of ozone in these regions. Because of the increase of ozone in the Arctic lower stratosphere in the two NCAR models (Figure 1a), warming occurs at these two models (Figures 3a and 3d), in contrast to the cooling in the other three models. The tropical tropopause temperature (averaged within 20°S/N) near 100 hPa is

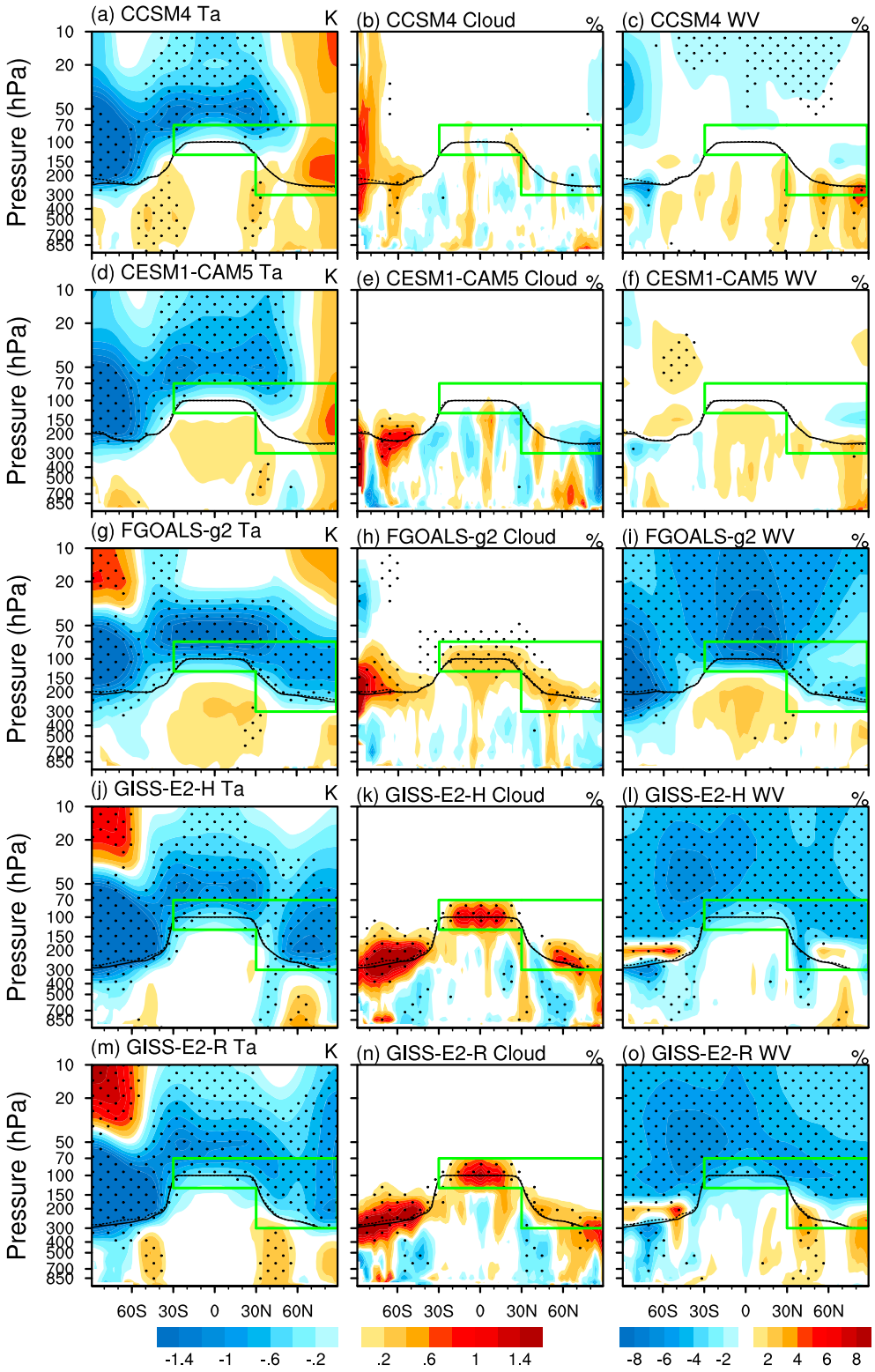

Figure 3. Annual and zonal mean responses from 1950–1959 to 1995–2004 in (a–c) CCSM4, (d–f) CESM1-CAM5, (g–i) FGOALS-g2, (j–l) GISS-E2-H, and (m–o) GISS-E2-R models. Panels in the left column show the temperature responses, units: kelvin. The middle column indicates the responses of cloud fraction, units: percent. Panels in the right column show the fractional changes in water vapor, units: percent. Regions with dots are the places where differences have statistical significant levels higher than the 95% confidence level (absolute values of student's t test are greater than 2.3). The green polygons mark the same region as in Figure 1.

noticeably decreased in FGOALS-g2, GISS-E2-H, and GISS-E2-R (−0.58 K, −0.34 K, and −0.36 K, respectively; see Figures 3g, 3j, and 3m) due to the reduction of ozone near the tropopause in these models (Figures 1b and 1c); this cooling is apparently much stronger than those in NCAR CCSM4 and CESM1-CAM5 (−0.04 K and −0.02 K, respectively).

Temperature changes near tropopause modify the local relative humidity and static stability, which can strongly impact the high clouds. The SH lower stratospheric cooling occurs in all the five models, which leads to increases in the relative humidity and decreases in the static stability near the tropopause and thus an increase of high clouds in the SH UTLS region. Similarly, the cooling above the tropical tropopause leads to a global increase of high clouds in FGOALS-g2, GISS-E2-H, and GISS-E2-R (Figures 3h, 3k, and 3n). However, the warming that occurs only in CCSM4 and CESM1-CAM5 in the NH extratropical lower stratosphere leads to reduction in high clouds in these two models (Figures 3b and 3e). Because of the greenhouse effect of high cloud, it can be deduced that the cloud longwave forcing associated with ozone change should be stronger in FGOALS-g2, GISS-E2-H, and GISS-E2-R than that in the NCAR models.

It is generally accepted that stratospheric water vapor is constrained by the tropical tropopause temperature (Fueglistaler et al., 2005; Randel et al., 2004). It is seen here that the UTLS ozone, via affecting the tropical tropopause temperature, influences the stratospheric water vapor. The stratospheric water vapor significantly decreases in the FGOALS-g2 and GISS models (Figures 3i, 3l, and 3o) because of the significant cooling of tropical tropopause (Figures 3g, 3j, and 3m). In contrast, it is a weak decrease in CCSM4 (Figure 3c), and a weak increase in CESM1-CAM5 (Figure 3f), which is consistent with the corresponding tropical tropopause temperature changes in these models. Stratospheric water vapor affects stratospheric temperature and chemistry (Forster & Shine, 2002; Shindell, 2001) and may also have implications for the rate of global surface warming (Solomon et al., 2010). Compared to the NCAR models, the strong stratospheric drying in the FGOALS-g2 and GISS models indicates that the potential climatic consequences related to water vapor may vary considerably among these models (Huang et al., 2016).

3.2. CAM5

The experiments performed with CAM5 are intent to verify the climate effects of the UTLS ozone, which are found by the comparisons of CMIP5 models. As shown in section 2.2, the O3A experiment corresponds to the experiments by the NCAR models (CCSM4 and CESM1-CAM5), and the O3B experiment corresponds to the experiments by the FGOLGS-g2 and GISS models.

Because the SST is fixed in these simulations, the responses to the ozone changes in the CAM5 experiments can be categorized as climate "adjustments" (Sherwood et al., 2015). As shown in Figure 4a, cooling occurs in the tropical and SH lower stratosphere, and warming occurs in the Arctic lower stratosphere in the O3A experiment. The temperature near tropopause, due to the counteracting effects of upper-level ozone decrease and local ozone increase (Lin et al., 2017), changes little in the tropics and NH midlatitudes in the O3A experiment. The change of the tropical tropopause temperature is about +0.04 K. This is consistent with the results from the CMIP5 CESM1-CAM5 (Figure 3d). There are a cooling-induced increase of high clouds over the Antarctic and a warming-induced decrease of high clouds over the Arctic in the O3A experiment (see Figures 4b and S1a and S1b in the supporting information). The stratospheric water vapor increase is mainly located in the middle stratosphere in this experiment (Figure 4c), which may result from the enhanced tropical upwelling in the stratosphere (Figure S1c).

As the sign of the tropical and NH UTLS ozone change is reversed in the O3B experiment, the UTLS ozone decreases result in a significant cooling near the tropopause in the tropics and NH midlatitudes (Figure 4d). The tropical tropopause temperature significantly decreases by about 0.32 K. Because the ozone depletion in the Arctic lower stratosphere is weak in the O3B experiment, the Arctic stratospheric radiative cooling is counteracted by the adiabatic warming, especially in the spring time (see Figures S1f and S2). It is a statistically insignificant warming in the Arctic stratosphere. The cloud adjustment in the O3B experiment, an increase of high clouds except for the Arctic region (Figure 4e), is similar to the CMIP5 FGOALS-g2 and GISS models. The decrease of static stability in the upper troposphere and the increase of relative humidity in the extratropics contribute to this increase of high clouds (Figures S1d and S1e). The stratospheric water vapor is reduced by the cooling of the tropical tropopause in the O3B experiment (Figure 4f).

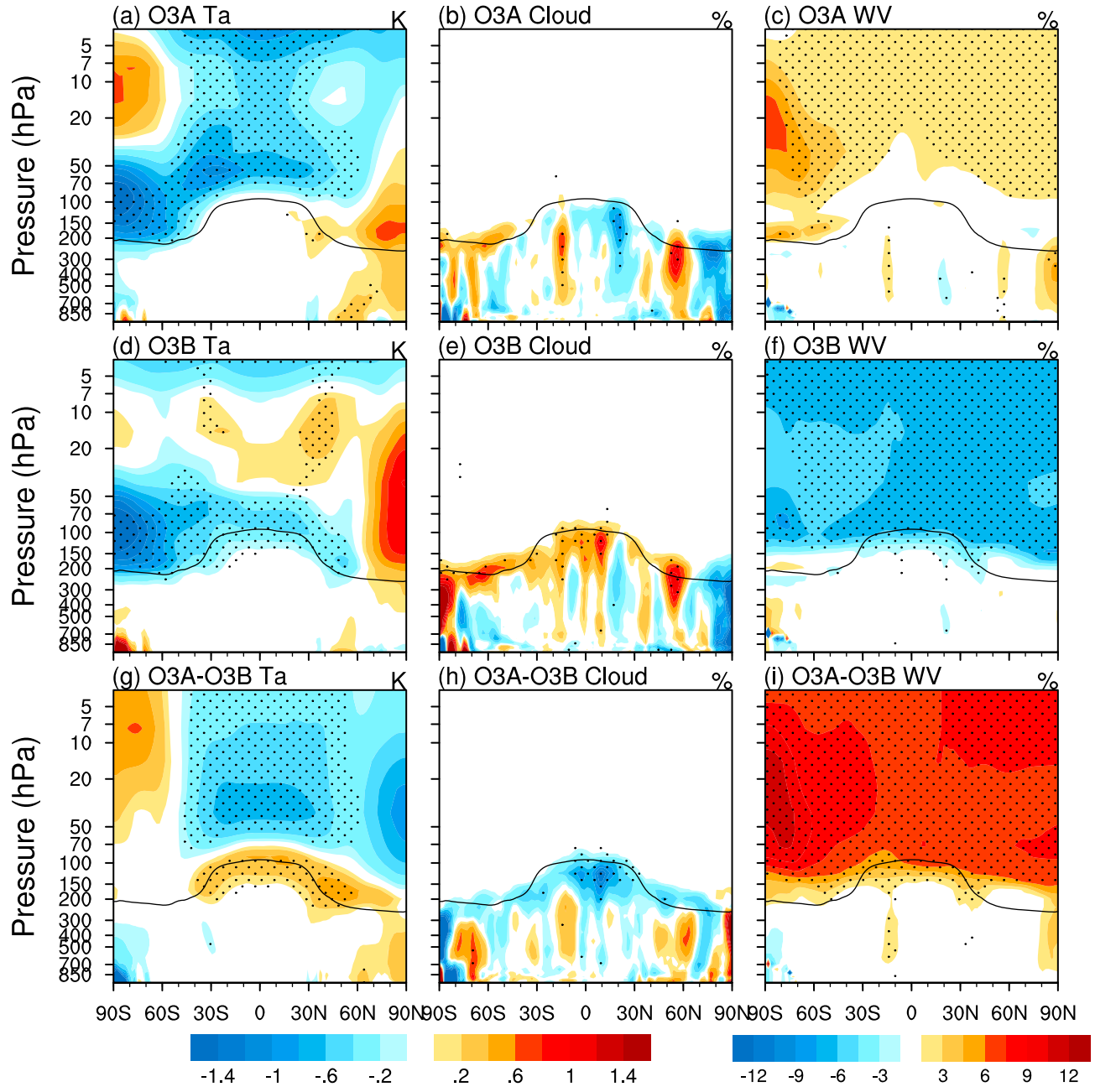

Figure 4. Annual and zonal mean responses in the (a–c) O3A, (d–f) O3B experiments, and (g–i) O3A-O3B. The panels in the left column show the temperature response, units: kelvin. The middle column indicates the responses of cloud fraction, units: percent. Panels in the right column show the fractional changes in water vapor, units: percent. Stippled are the regions where the differences are significant at the 95% confidence level.

By comparing the O3A and O3B experiments, it is clear that the UTLS ozone increase results in warming in the UTLS region and cooling in the stratosphere (Figure 4g), reduction of high clouds near the tropopause (Figure 4h), and moistening of stratosphere (Figure 4i). Although the ozone difference between the O3A and O3B experiments is an increase located mainly around the tropopause (Figure 3c), the stratospheric cooling difference mainly comes from the radiative cooling induced by the less longwave absorption by the stratospheric ozone, which is verified by the calculation using a rapid radiative transfer model, RRTM (a validated, correlated *k*-distribution band model) (Mlawer et al., 1997) (Figure 5a). The increase of the stratospheric water vapor also contributes to cooling the middle and upper stratosphere (Figure 5b). On the contrary, stratospheric temperature is not sensitive to the decrease of the high clouds (Figure 5c).

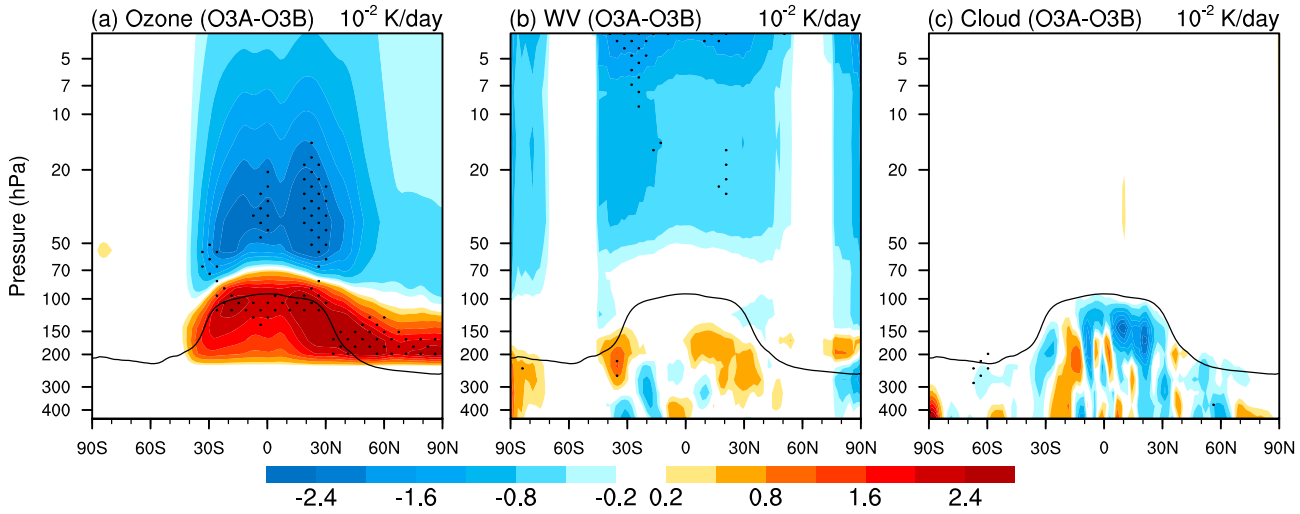

Figure 5. Annual and zonal mean changes of heating rates between the O3A and O3B experiments caused by the difference of (a) ozone, (b) water vapor, and (c) cloud. The heating rates are calculated with RRTM. Units: 10^{-2} K/d. Stippled are the regions where the differences are significant at the 95% confidence level.

To test the robustness of the results, the control, O3A, and O3B experiments are also performed with a coupled ocean-atmosphere model, CESM1.2-CAM5. Because of the small radiative forcing of ozone changes, the global and annual mean surface temperature changes little in the O3A and O3B experiments (about −0.1 K and −0.2 K, respectively). The responses to UTLS ozone increase, including stratospheric cooling, reduction of high clouds, and moistening of stratosphere, are consistent with those in the fixed-SST experiments (see Figure S3).

Radiative impacts are calculated for the climate adjustments associated with the ozone changes. First, we calculate the instantaneous radiative forcing (F_i) of ozone change at the top of atmosphere (TOA), which denotes the instantaneous change of TOA radiation fluxes in response to the ozone change, using RRTM. Then, we analyze the TOA radiative flux changes due to stratospheric temperature, stratospheric water vapor, clouds, and tropospheric temperature and water vapor using the TOA kernels introduced by Huang et al. (2017). The analysis method follows Xia et al. (2016). The radiative effects of temperature and water vapor are calculated as $\Delta R_V = \frac{\partial R}{\partial V}\Delta V$, where $\frac{\partial R}{\partial V}$ is the precalculated radiative sensitivity kernel in Huang et al. (2017) and ΔV is the change of the climate variable, such as temperature, water vapor, and surface albedo in response to ozone change in the O3A and O3B experiments, respectively. By comparing the climate adjustments to the instantaneous radiative forcing, we can make clear how do these climate processes modify the direct climate effect of the ozone change.

The global and annual mean instantaneous radiative forcing of ozone change is −0.16 and −0.27 W m^{-2} in the O3A and O3B experiments, respectively. This forcing is further modified by various adjustments. Because of the stronger stratospheric cooling resulted from the more UTLS ozone in the O3A experiment, the stratospheric temperature adjustment is 0.07 W m^{-2} larger than that in the O3B experiment. The direct radiative

Table 1
Global and Annual Mean TOA Radiative Forcing and Adjustments

	F_i	Stratospheric temperature	Stratospheric water vapor	Cloud longwave effect	Cloud short wave effect	Tropospheric temperature and water vapor	F_e
O3A	−0.16	0.12	0.00	−0.08	0.18	−0.06	0.00
O3B	−0.27	0.05	0.00	0.07	0.07	−0.08	−0.16
O3A − O3B	0.11	0.07	0.00	−0.15	0.11	0.02	0.16

Note. The columns indicate the instantaneous radiative forcing of ozone and the radiation changes caused by stratospheric temperature, stratospheric water vapor, cloud longwave effect, cloud shortwave effect, and tropospheric temperature and water vapor, respectively. The last column is the effective forcing (sum of all the preceding columns). Units: W m^{-2}.

effect of stratospheric water vapor is negligible in both experiments. The cloud longwave adjustment, mainly resulting from changes in the high and middle clouds, is −0.08 and 0.07 W m^{-2} in the O3A and O3B experiments, respectively. The difference between the O3A and O3B experiments, which indicates the effect of the UTLS ozone increase, has an instantaneous radiative forcing of about 0.11 W m^{-2}. The cloud longwave adjustment associated with the UTLS ozone increase is −0.15 W m^{-2}. The adjustment of the stratospheric temperature, directly caused by the UTLS ozone increase, is 0.07 W m^{-2}. These results affirm that the climate adjustments have similar magnitudes to the instantaneous forcing and can strongly modify the climatic effects of stratospheric ozone, which is consistent with the finding of Xia et al. (2016). The effective radiative forcing (F_e), which consists of F_i and all the adjustments (stratospheric temperature and water vapor, clouds, tropospheric temperature and water vapor), is 0.00 and −0.16 W m^{-2} in the O3A and O3B experiments, respectively (Table 1).

4. Conclusions and Discussions

In this study, we analyze the climate responses to different distributions of ozone changes, especially in the UTLS region, using the CMIP5 ozone-only historical experiments and the experiments of a latest GCM, CAM5. We find that the high clouds and stratospheric temperature and water vapor are sensitive to the UTLS ozone change and strongly modify the radiative forcing of ozone.

Among the CMIP5 models analyzed, the GCMs with UTLS ozone reduction in all the latitudes (the FGOALS-g2 and GISS models) project a global increase of high clouds and a significant reduction of stratospheric water vapor. The significant (95% confidence level) increases of the high clouds can reach about 0.4% in the FGOALS-g2 and 1.4% in the GISS models. And the total mass of the stratospheric water vapor significantly decreases by about 4.4% and 3.5% in the FGOALS-g2 and GISS models, respectively. In contrast, the NCAR models (CCSM4 and CESM1-CAM5) in which the UTLS ozone increases in the tropics and NH extratropics project an insignificant change of high clouds in these latitudes and little stratospheric water vapor change (−0.3% and 0.4%, respectively). The high cloud change results from the UTLS temperature changes that affect local relative humidity and static stability (Hansen et al., 1997; Hodnebrog et al., 2014; Xia et al., 2016). The changes of high clouds in the tropical tropopause layer is well explained by the vertical temperature gradient (static stability), which is consistent with the results in Tseng and Fu (2017). Stratospheric water vapor is mainly controlled by the tropical tropopause temperature (Fueglistaler et al., 2005; Randel et al., 2004). The UTLS ozone, via influencing the UTLS temperature, strongly modifies the high clouds near the tropopause and overall water vapor amount in the stratosphere.

The impacts of the UTLS ozone change on the high clouds and stratospheric water vapor are verified by a set of CAM5 experiments. The simulations with contrasting changes in UTLS ozone (the O3A and O3B experiments) generally reproduce the responses of both high clouds and stratospheric water vapor in the CMIP5 models. By comparing the O3A to O3B experiments, we affirm the effects of the UTLS ozone increase which leads to stratospheric cooling, reduction of high clouds, and increase of stratospheric water vapor. The climate adjustments associated with the increase of UTLS ozone are −0.15 W m^{-2} for the reduction of high clouds, and 0.07 W m^{-2} for the stratospheric cooling. The magnitudes of these adjustments are comparable to the instantaneous forcing of the stratospheric ozone change.

The results here point out the importance of the UTLS ozone changes during climate change, which are consistent with the previous studies (Forster & Shine, 1997; Lacis et al., 1990; Riese et al., 2012), in which the direct radiative effect of the UTLS ozone is highlighted. To better understand how the tropospheric and surface climate respond to ozone change, such as in the studies of ozone depletion in the 20th century and recovery in the 21st century, we need to pay attention to the UTLS region. And further studies are needed to better understand the uncertainties in the observed UTLS ozone trends and improve the ozone data sets. Whether the future experiments in CMIP6 use prescribed ozone distribution or interactive chemistry, it is important to elucidate the intermodel discrepancies in climate responses due to spatial differences of ozone changes.

Acknowledgments
We thank Jian Yue, Qiang Fu, and Kevin Grise for helpful comments. The data used are listed in the references, figures, and tables. Y. Huang is supported by grants from the Discovery Program of the Natural Sciences and Engineering Council of Canada (RGPIN 418305-13) and the Team Research Project Program of the Fonds de recherché Nature et technologies of Quebec (PR-190145). Y. Hu is supported by the Natural Science Foundation of China, under grants 41375072 and 41530423.

References

Arblaster, J. M., Meehl, G. A., & Karoly, D. J. (2011). Future climate change in the Southern Hemisphere: Competing effects of ozone and greenhouse gases. *Geophysical Research Letters*, *38*, L02701. https://doi.org/10.1029/2010GL045384

Bekki, S., Bodeker, G. E., Bais, A. F., Butchart, N., Eyring, V., Fahey, D. W., … Shibata, K. (2011). Future ozone and its impact on surface UV. In *Scientific assessment of ozone depletion: 2010, Global Ozone Research and Monitoring Project—Report No. 52* (Chap. 3, pp. 516). Geneva, Switzerland: World Meteorological Organization.

Bitz, C. M., & Polvani, L. M. (2012). Antarctic climate response to stratospheric ozone depletion in a fine resolution ocean climate model. *Geophysical Research Letters*, *39*, L20705. https://doi.org/10.1029/2012GL053393

Butchart, N., Scaife, A. A., Bourqui, M., de Grandpré, J., Hare, S. H. E., Kettleborough, J., … Sigmond, M. (2006). Simulations of anthropogenic change in the strength of the Brewer–Dobson circulation. *Climate Dynamics*, *27*(7-8), 727–741. https://doi.org/10.1007/s00382-006-0162-4

Cheung, J. C. H., Haigh, J. D., & Jackson, D. R. (2014). Impact of EOS MLS ozone data on medium-extended range ensemble weather forecasts. *Journal of Geophysical Research: Atmospheres*, *119*, 9253–9266. https://doi.org/10.1002/2014JD021823

Chiodo, G., & Polvani, L. M. (2017). Reduced Southern Hemispheric circulation response to quadrupled CO_2 due to stratospheric ozone feedback. *Geophysical Research Letters*, *44*, 465–474. https://doi.org/10.1002/2016GL071011

Collins, W. D., Rasch, P. J., Boville, B. A., Hack, J. J., McCaa, J. R., Williamson, D. L., … Zhang, M. H. (2006). The formulation and atmospheric simulation of the Community Atmosphere Model version 3 (CAM3). *Journal of Climate*, *19*(11), 2144–2161. https://doi.org/10.1175/JCLI3760.1

Eyring, V., Arblaster, J. M., Cionni, I., Sedláček, J., Perlwitz, J., Young, P. J., … Watanabe, S. (2013). Long-term ozone changes and associated climate impacts in CMIP5 simulations. *Journal of Geophysical Research: Atmospheres*, *118*, 5029–5060. https://doi.org/10.1002/jgrd.50316

Forster, P. M., & Shine, K. P. (1997). Radiative forcing and temperature trends from stratospheric ozone changes. *Journal of Geophysical Research*, *102*(D9), 10,841–10,855. https://doi.org/10.1029/96JD03510

Forster, P. M. D. F., & Shine, K. P. (2002). Assessing the climate impact of trends in stratospheric water vapor. *Geophysical Research Letters*, *29*(6), 1086. https://doi.org/10.1029/2001GL013909

Fu, Q., Lin, P., Solomon, S., & Hartmann, D. L. (2015). Observational evidence of strengthening of the Brewer-Dobson circulation since 1980. *Journal of Geophysical Research: Atmospheres*, *120*, 10,214–10,228. https://doi.org/10.1002/2015JD023657

Fueglistaler, S., Bonazzola, M., Haynes, P. H., & Peter, T. (2005). Stratospheric water vapor predicted from the Lagrangian temperature history of air entering the stratosphere in the tropics. *Journal of Geophysical Research*, *110*, D08107. https://doi.org/10.1029/2004JD005516

Gettelman, A., Hegglin, M. I., Son, S. W., Kim, J., Fujiwara, M., Birner, T., … Tian, W. (2010). Multimodel assessment of the upper troposphere and lower stratosphere: Tropics and global trends. *Journal of Geophysical Research*, *115*, D00M08. https://doi.org/10.1029/2009JD013638

Hansen, J., Sato, M., & Ruedy, R. (1997). Radiative forcing and climate response. *Journal of Geophysical Research*, *102*(D6), 6831–6864. https://doi.org/10.1029/96JD03436

Harris, N. R. P., Hassler, B., Tummon, F., Bodeker, G. E., Hubert, D., Petropavlovskikh, I., … Zawodny, J. M. (2015). Past changes in the vertical distribution of ozone—Part 3: Analysis and interpretation of trends. *Atmospheric Chemistry and Physics*, *15*(17), 9965–9982. https://doi.org/10.5194/acp-15-9965-2015

Hegglin, M. I., Gettelman, A., Hoor, P., Krichevsky, R., Manney, G. L., Pan, L. L., … Yamashita, Y. (2010). Multimodel assessment of the upper troposphere and lower stratosphere: Extratropics. *Journal of Geophysical Research*, *115*, D00M09. https://doi.org/10.1029/2010JD013884

Hodnebrog, Ø., Myhre, G., & Samset, B. H. (2014). How shorter black carbon lifetime alters its climate effect. *Nature Communications*, *5*, 5065. https://doi.org/10.1038/ncomms6065

Hu, Y., & Fu, Q. (2009). Stratospheric warming in Southern Hemisphere high latitudes since 1979. *Atmospheric Chemistry and Physics*, *9*(13), 4329–4340. https://doi.org/10.5194/acp-9-4329-2009

Hu, Y., & Xia, Y. (2013). Extremely cold and persistent stratospheric Arctic vortex in the winter of 2010–2011. *Chinese Science Bulletin*, *58*(25), 3155–3160. https://doi.org/10.1007/s11434-013-5945-5

Huang, Y., Xia, Y., & Tan, X. (2017). On the pattern of CO_2 radiative forcing and poleward energy transport. *Journal of Geophysical Research: Atmospheres*, *122*, 10,578–10,593. https://doi.org/10.1002/2017JD027221

Huang, Y., Zhang, M. H., Xia, Y., Hu, Y. Y., & Son, S. W. (2016). Is there a stratospheric radiative feedback in global warming simulations? *Climate Dynamics*, *46*(1-2), 177–186. https://doi.org/10.1007/s00382-015-2577-2

Kang, S. M., Polvani, L. M., Fyfe, J. C., & Sigmond, M. (2011). Impact of polar ozone depletion on subtropical precipitation. *Science*, *332*(6032), 951–954. https://doi.org/10.1126/science.1202131

Karpechko, A. Y., Perlwitz, J., & Manzini, E. (2014). A model study of tropospheric impacts of the Arctic ozone depletion 2011. *Journal of Geophysical Research: Atmospheres*, *119*, 7999–8014. https://doi.org/10.1002/2013JD021350

Lacis, A. A., Wuebbles, D. J., & Logan, J. A. (1990). Radiative forcing of climate by changes in the vertical-distribution of ozone. *Journal of Geophysical Research*, *95*(D7), 9971–9981. https://doi.org/10.1029/JD095iD07p09971

Lamarque, J. F., Bond, T. C., Eyring, V., Granier, C., Heil, A., Klimont, Z., … van Vuuren, D. P. (2010). Historical (1850–2000) gridded anthropogenic and biomass burning emissions of reactive gases and aerosols: Methodology and application. *Atmospheric Chemistry and Physics*, *10*(15), 7017–7039. https://doi.org/10.5194/acp-10-7017-2010

Lamarque, J.-F., Kyle, G. P., Meinshausen, M., Riahi, K., Smith, S. J., van Vuuren, D. P., … Vitt, F. (2011). Global and regional evolution of short-lived radiatively-active gases and aerosols in the Representative Concentration Pathways. *Climatic Change*, *109*(1-2), 191–212. https://doi.org/10.1007/s10584-011-0155-0

Lin, P., & Fu, Q. (2013). Changes in various branches of the Brewer–Dobson circulation from an ensemble of chemistry climate models. *Journal of Geophysical Research: Atmospheres*, *118*, 73–84. https://doi.org/10.1029/2012JD018813

Lin, P., Paynter, D., Ming, Y., & Ramaswamy, V. (2017). Changes of the tropical tropopause layer under global warming. *Journal of Climate*, *30*(4), 1245–1258. https://doi.org/10.1175/jcli-d-16-0457.1

Manney, G. L., Santee, M. L., Rex, M., Livesey, N. J., Pitts, M. C., Veefkind, P., … Zinoviev, N. S. (2011). Unprecedented Arctic ozone loss in 2011. *Nature*, *478*(7370), 469–475. Retrieved from http://www.nature.com/nature/journal/v478/n7370/abs/nature10556.html#supplementary-information, https://doi.org/10.1038/nature10556

Mlawer, E. J., Taubman, S. J., Brown, P. D., Iacono, M. J., & Clough, S. A. (1997). Radiative transfer for inhomogeneous atmospheres: RRTM, a validated correlated-k model for the longwave. *Journal of Geophysical Research*, *102*(D14), 16,663–16,682. https://doi.org/10.1029/97JD00237

Neale, R. B., Chen, C.-C., Gettelman, A., Lauritzen, P. H., Park, S., Williamson, D. L., & Lamarque, J.-F. (2010). Description of the NCAR community atmosphere model (CAM 5.0), NCAR Tech. Note NCAR/TN-486+ STR.

Perlwitz, J., Pawson, S., Fogt, R. L., Nielsen, J. E., & Neff, W. D. (2008). Impact of stratospheric ozone hole recovery on Antarctic climate. *Geophysical Research Letters*, *35*, L08714. https://doi.org/10.1029/2008GL033317

Ploeger, F., Konopka, P., Günther, G., Grooß, J. U., & Müller, R. (2010). Impact of the vertical velocity scheme on modeling transport in the tropical tropopause layer. *Journal of Geophysical Research*, *115*, D03301. https://doi.org/10.1029/2009JD012023

Randel, W. J., Wu, F., Oltmans, S. J., Rosenlof, K., & Nedoluha, G. E. (2004). Interannual changes of stratospheric water vapor and correlations with tropical tropopause temperatures. *Journal of the Atmospheric Sciences*, *61*(17), 2133–2148. https://doi.org/10.1175/1520-0469(2004)061%3C2133:icoswv%3E2.0.co;2

Riese, M., Ploeger, F., Rap, A., Vogel, B., Konopka, P., Dameris, M., & Forster, P. (2012). Impact of uncertainties in atmospheric mixing on simulated UTLS composition and related radiative effects. *Journal of Geophysical Research*, *117*, D16305. https://doi.org/10.1029/2012JD017751

Roth, C., Degenstein, D. A., & Bourassa, A. E. (2014). Trends in stratospheric ozone derived from merged Odin-OSIRIS and SAGE II satellite observations. *Atmospheric Chemistry and Physics*, *14*(6), 7113–7140.

Shepherd, T. G., & McLandress, C. (2011). A robust mechanism for strengthening of the Brewer–Dobson circulation in response to climate change: Critical-layer control of subtropical wave breaking. *Journal of the Atmospheric Sciences*, *68*(4), 784–797. https://doi.org/10.1175/2010jas3608.1

Sherwood, S. C., Bony, S., Boucher, O., Bretherton, C., Forster, P. M., Gregory, J. M., & Stevens, B. (2015). Adjustments in the forcing-feedback framework for understanding climate change. *Bulletin of the American Meteorological Society*, *96*(2), 217–228. https://doi.org/10.1175/bams-d-13-00167.1

Shindell, D. T. (2001). Climate and ozone response to increased stratospheric water vapor. *Geophysical Research Letters*, *28*(8), 1551–1554. https://doi.org/10.1029/1999GL011197

Solomon, S. (1999). Stratospheric ozone depletion: A review of concepts and history. *Reviews of Geophysics*, *37*(3), 275–316. https://doi.org/10.1029/1999RG900008

Solomon, S., Rosenlof, K. H., Portmann, R. W., Daniel, J. S., Davis, S. M., Sanford, T. J., & Plattner, G. K. (2010). Contributions of stratospheric water vapor to decadal changes in the rate of global warming. *Science*, *327*(5970), 1219–1223. https://doi.org/10.1126/science.1182488

Son, S.-W., Polvani, L. M., Waugh, D. W., Akiyoshi, H., Garcia, R., Kinnison, D., … Shibata, K. (2008). The impact of stratospheric ozone recovery on the southern hemisphere westerly jet. *Science*, *320*(5882), 1486–1489. https://doi.org/10.1126/science.1155939

Son, S.-W., Tandon, N. F., Polvani, L. M., & Waugh, D. W. (2009). Ozone hole and Southern Hemisphere climate change. *Geophysical Research Letters*, *36*, L15705. https://doi.org/10.1029/2009GL038671

Steinbrecht, W., Froidevaux, L., Fuller, R., Wang, R., Anderson, J., Roth, C., … Tummon, F. (2017). An update on ozone profile trends for the period 2000 to 2016. *Atmospheric Chemistry and Physics*, *17*(17), 10,675–10,690. https://doi.org/10.5194/acp-17-10675-2017

Taylor, K. E., Stouffer, R. J., & Meehl, G. A. (2012). An overview of CMIP5 and the experiment design. *Bulletin of the American Meteorological Society*, *93*(4), 485–498. https://doi.org/10.1175/bams-d-11-00094.1

Thompson, D. W. J., Solomon, S., Kushner, P. J., England, M. H., Grise, K. M., & Karoly, D. J. (2011). Signatures of the Antarctic ozone hole in Southern Hemisphere surface climate change. *Nature Geoscience*, *4*(11), 741–749. https://doi.org/10.1038/ngeo1296

Tseng, H.-H., & Fu, Q. (2017). Temperature control of the variability of tropical tropopause layer cirrus clouds. *Journal of Geophysical Research: Atmospheres*, *122*, 11,062–11,075. https://doi.org/10.1002/2017JD027093

Turner, J., Comiso, J. C., Marshall, G. J., Lachlan-Cope, T. A., Bracegirdle, T., Maksym, T., … Orr, A. (2009). Non-annular atmospheric circulation change induced by stratospheric ozone depletion and its role in the recent increase of Antarctic sea ice extent. *Geophysical Research Letters*, *36*, L08502. https://doi.org/10.1029/2009GL037524

Xia, Y., Hu, Y., & Huang, Y. (2016). Strong modification of stratospheric ozone forcing by cloud and sea-ice adjustments. *Atmospheric Chemistry and Physics*, *16*(12), 7559–7567. https://doi.org/10.5194/acp-16-7559-2016

Xie, F., Li, J., Tian, W., Fu, Q., Jin, F., Hu, Y., … Feng, J. (2016). A connection from Arctic stratospheric ozone to El Niño-Southern Oscillation. *Environmental Research Letters*, *11*(12), 124026. https://doi.org/10.1088/1748-9326/11/12/124026

Xie, F., Tian, W., & Chipperfield, M. P. (2008). Radiative effect of ozone change on stratosphere-troposphere exchange. *Journal of Geophysical Research*, *113*, D00B09. https://doi.org/10.1029/2008JD009829

Zhang, J., Tian, W., Chipperfield, M. P., Xie, F., & Huang, J. (2016). Persistent shift of the Arctic polar vortex towards the Eurasian continent in recent decades. *Nature Climate Change*, *6*(12), 1094–1099. https://doi.org/10.1038/nclimate3136, http://www.nature.com/nclimate/journal/v6/n12/abs/nclimate3136.html#supplementary-information